 CMC, vol.36, no.3, pp.257-270, 2013

Numerical Evaluation of Variation in 'Characteristic Distance' due to Fracture Specimen Thickness and Temperature

Sanjeev Saxena[1], **Raghvendra Singh**[2], **Geeta Agnihotri**[2]

Abstract: The present numerical study is an attempt to understand the dependency of characteristic distance on the fracture specimen thickness and temperature. The presented work will be useful to establish the characteristic distance prediction methodology using three dimensional FEM model. Based on the methods proposed for the numerical prediction of characteristic distance, it comes out that it depends on fracture specimen thickness and finally it converges after a specified thickness of fracture specimen. In Armco iron material, characteristic distance varies in temperature ranges where dynamic strain ageing phenomenon is observed, initially decrease and then increases again.

Keywords: FEM, characteristic distance, process zone, thickness, high temperature.

1 Introduction

In most design situations a material that demonstrates ductile fracture is usually preferred for the reason that ductile materials plastically deform, thereby slowing down the process of fracture and giving ample time for the problem to be corrected. Industries like aerospace, automobile and power plants are increasingly demanding highly tough ductile materials to optimize the component dimensions without reducing the safety margins. Thus it is indispensable that the nonlinear properties of the used materials be known and modeled precisely (Miguel et el., 2010), especially the fracture behaviour of ductile material (khedle et al., 2011; Panthi and Saxena, 2012). In ductile materials the crack growth mechanism is considered to be due to void nucleation, growth and final coalescence with the crack tip. The fracture parameters which are usually used to define the crack growth behaviour of ductile

[1] CSIR-Advanced Materials and Processes Research Institute, Hoshangabad Road, Bhopal - 462 064, India.
[2] Maulana Azad National Institute of Technology, Bhopal- 603 102, India.

material are: stress intensity factor (K), energy release rate (G), crack tip opening displacement (CTOD) and J-integral (J). Along with these there is another fracture parameter called 'characteristic distance' (lc) or process zone. The lc is defined as the distance between the crack tip and the void responsible for eventual coalescence with the crack tip. Although approximate, lc assumes a special significance as it links the fracture behaviour to the microscopic mechanism considered responsible for ductile fracture. Fracture behaviour of ductile material is also shown in terms of crack growth resistance curve given by elastic-plastic J-resistance curve ($J-$R curve). Generally material $J-$R curve is obtain experimentally using fracture test results of standard fracture specimens (CT, TPB etc.). The crack growth behaviour of ductile material is also numerically predicted using damage mechanics principles (Saxena et al., 2010(a); Tserpes and Koumpias, 2012). Using damage mechanics principles, the knowledge of the lc is crucial for designing the size of finite element mesh in the numerical simulation of crack growth.

Conceptually, these fracture parameters should be an intrinsic material property that should not vary with changes in specimen size, crack length, thickness of material etc. The geometry dependency of some of these fracture parameters (K_{1C}, J_{1C} and J_{szw}) has been shown both experimentally (Narasaiah et al., 2010) and numerically (Saxena et al., 2010(b)) in the literature. This been the reason ASTM code (ASTI-E1820, 2011) specified the fracture specimen dimensions criteria to be meet out for the geometry independent experimental evaluation of these fracture parameters. Experimental and numerical (using two dimensional FEM model) evaluation of lc has been reported in the literature (Ramakrishnan and RamaRao, 2005; Saxena and Ramakrishnan, 2007). Both experimental evaluation and numerical prediction of lc dependency on the fracture specimen geometry and temperature is not reported in the literature. The presented work is an attempt to understand numerically, the geometry dependency of lc using three-dimensional FEM analysis. To study the dependency of lc on temperature, the present numerical study has also been extended to Armco iron tested (Srinivas et al., 1993-1994) at different temperatures (298°K, 383°K, 423°K, 473°K, and 573°K). In Armco iron material, experimentally determined (Srinivas et al., 1993-1994) value of lc at room temperature is numerically predicted. Assessment of variation in lc parameter across the fracture specimen thickness is useful to establish lc prediction methodology using 3D FEM model. In terms of lc, the fracture specimen thickness requirement given in ASTM, to obtain valid (geometry independent) fracture parameter, is also evaluated. Presented work will be helpful in establishing lc as a valid fracture parameter.

2 Characteristic distance (lc) as fracture parameter

Orowan formulate a hypothesis on the possibility of fracture initiation at a certain distance ahead of the notch tip (Orowan,1948). This concept implies that void nucleation occur at a distance from the crack tip and further growth of micro crack is in the direction opposite to that of the main crack resulting in final coalescence with the crack tip. There are also experimental evidences in fractographic investigation supporting to it. Generally, for elastic-plastic conditions two parameter concepts is initially proposed. This incorporates measurement of critical stress parameter at a distance (characteristic distance) ahead of crack tip where initiation of fracture occurs. The experimental evidences also provide fact about the size of lc of the order of material's grain size (greater or equal to grain size). Thus lc is considered related to some structural element such as material's grain size (Krasowsky and Pluvinage, 1996).

Several works has been done to understand and evaluate lc through experimental and numerical means. Nakamura et al. (1995) carried out a 2D FEM analyses taking into account lc as a parameter. Using uni-axial stress assumption, Zhiming (1998) presented a derivation on the size of fracture process zone. Zhao et al. (2000) carried out parametric study on the growing crack tip field and also predicted the shapes of process zone. Wnuk et al. (2002) found that the variations in microstructural parameters strongly affect the lc and are the characteristics of stress induced in the vicinity of the crack front, which can be represented by stress triaxiality parameter. While simulating crack growth behaviour, there are also attempts (Matvienko, 2004; Yan-qing and Zhang 2006; Yang and Shiva, 2011; Sarris and Papanastasiou, 2011) to understand process zone using cohesive approach in 2D FEM models. Frank Vernerey (2009) also used finite element formulation with considering failure mechanism concentrating within a region of characteristic distance. Using transmission-optical microscopy, Du et al. (1998) studied the effect of process zone on toughness and the evolution of process zone. Hadjab et al. (2007) used experimental techniques like SEM to develop understanding of the micro level aspect within characteristic distance. Volokh (2011) experimentally found that damage localize in a narrow zone of characteristic distance from where the initiation of crack occurs. Using both experimental and numerical tools, Wang et al. (2002) studied lc and its dependency on temperature variation. Similarly, using both techniques Haider (2005) examine the effect of specimen size on the process zone. Using the same tools, Jones et al. (2007) try to study the variation in size of process zone due to high energy X ray source. In brittle material, Xiaozhi and Kai (2007) studies the effect of size on the material strength, which is found to be due to the interaction of parameters within the fracture process zone. Thus, the numerical prediction of lc using 3D FEM model and its dependency on fracture specimen

thickness and temperature is not reported in the literature. Using Armco iron tested data the present work is an attempt towards that. The knowledge of the 'lc' is also crucial for the finite element simulations of material failure because it provides the otherwise missing physical length-scale over which continuum damage occurs otherwise the crack growth simulation results could consider as mesh dependent. The latter means that the 'lc' sets the size of the finite elements that should be used for the material in the areas where failure propagates.

3 Experimentally tested data used

Tensile tests and fracture toughness (J_{SZW}) tests data of Armco iron (grain size 78 μm) material tested at temperatures ranging from 298°K to 573°K are taken from literature (Srinivas, 1993). Cylindrical tensile specimens of 15 mm gauge length and 4.5 mm gauge diameter had been used and these were tested at a nominal strain rate of 10^{-3} s^{-1}. For the material, the ductile fracture toughness (J_{SZW}) was obtained using multiple specimens $J-R$curve technique. Compact tension specimens of 25 mm thickness were used at all the test temperatures except at 298°K (room) temperature at which 50 mm thick specimens were utilized. Experimentally lc was obtained at room temperature using the SEM micrographs of the sectioned surfaces of interrupted test samples as reported in (Srinivas, 1994). The results of tensile and fracture tests for the material tested at different temperatures is given in Table 1.

Table 1: Experimental tested data used in the numerical simulation

Temperature (Degree Kelvin)	E (GPa)	n	σ_y (MPa)	σ_u (MPa)	Critical energy density, $E_{Crit.}$ (MJ/m^3)	Fracture energy density, $E_{Fract.}$ (MJ/m^3)	J_{SZW} (N/mm)	lc (microns)
298	196	0.29	189	296	92	1357	165	110
383	191	0.30	151	338	105	1396	230	—-
423	187	0.41	150	385	148	1480	260	—-
473	180	0.48	148	404	183	1565	290	—-
573	175	0.38	146	404	154	1735	280	—-

4 Numerical prediction of 'characteristic distance' (lc)

In the present investigation three dimensional FEM analyses have been carried out using ABAQUS FEM software (2006). The predicted results are then evaluated to

assess 'characteristic distance'. The numerical predicted Lc value at room temperature is then validated with experimental results. The present numerical prediction of lc have been carried out using tensile tested data of Armco iron material tested at different temperatures (298^oK, 383^oK, 423^oK, 473^oK, and 573^oK). The numerical study have also been carried out using different thickness (3.125mm, 6.25mm, 12.5mm, 25mm, 50mm and 100mm thick) of standard compact tension (CT) specimens. Thus, the present study tries to explore the variation of lc due to change in temperature and fracture specimen thickness.

4.1 Numerical prediction methodology

'Characteristic distance' is numerically predicted using energy based methodology described in Saxena et al. (Saxena and Ramakrishnan (2007)) using *critical energy density* define on material's true stress strain tensile test data. Here, *critical energy density* is defined as the energy density integral at the critical strain (ε_c) corresponding to onset of necking in tensile specimen or strain hardening exponent (n) for the specific case of power law variation of material's true stress–strain curve, given as:

$$E_{Crit.} = \int_0^n \sigma d\varepsilon \tag{1}$$

where n is strain-hardening coefficient in power law, corresponding to onset of necking. As shown in Fig. 1, the highly deformed distance ahead of the blunted crack front delineated by *critical energy density* ($E_{Crit.}$) is numerically defined as characteristic distance.

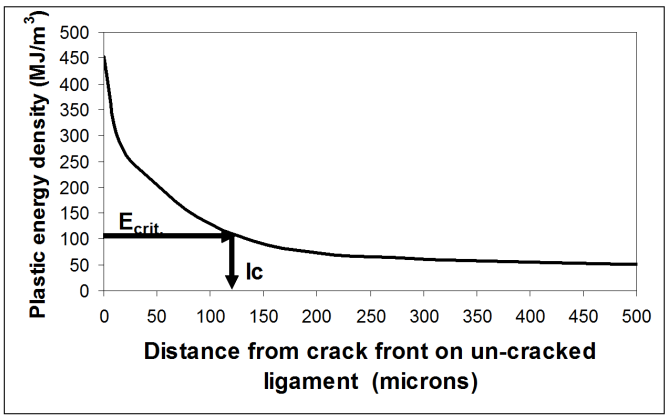

Figure 1: Numerical assessment of Characteristic distance at a plane ahead of crack front

With the increase in load line displacement (LLD), energy dissipation near the crack front increases and reaches a value corresponding to the material's *fracture energy density* (Saxena et al, 2009). The *fracture energy density* at which critical 'characteristic distance' (lc) is predicted, given as:

$$E_{Fract.} = \int_0^{\varepsilon_f} \sigma d\varepsilon \tag{2}$$

where ε_f is the fracture strain of the material.

Using the above two equations the two energy densities obtained for Armco iron material tested at different temperature are as given in Table 1.

4.2 Numerical FEM model

To have better understanding of the variation of lc across the thickness, three dimensional FEM model of CT specimen have been used. The investigation was limited to CT specimen analysis subjected to mode-I type of loading. The symmetry in this case permits consideration of only one fourth of the specimen geometry for computational economy. The analyses were done using commercial FEM software ABAQUS (ABAQUS, 2006). The mesh was constructed with eight noded brick elements with hourglass control as available in ABAQUS. Using two-dimensional FEM models, the convergence of FEM mesh for the given problem is established earlier (Saxena et al., 2009). Same mesh and size of elements is used in the cross section of 3D model as was used earlier (Saxena et al., 2009). Based on the convergence study conducted on 3D FEM model (half thickness), ten elements in the thickness direction was found to give reasonably good converged results. A typical FEM mesh used in the CT fracture specimen model (one-fourth) is shown in Fig. 2.

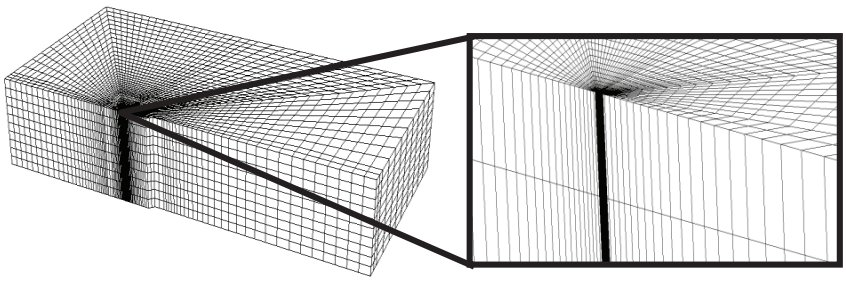

Figure 2: Typical FEM model of CT specimen and mesh near the crack front

Using $E_{Crit.}$, two dimensional FEM models and experimentally tested data of different grain size of Armco iron, the numerical prediction methodology of lc is vali-

dated earlier (Saxena and Ramakrishnan, 2007). In the present study the numerical prediction methodology of lc is further establish using both $E_{Crit.}$ and $E_{Fract.}$and 3D FEM model results. To validate this numerical methodology using 3D FEM model, 298°K (room) temperature test results of Armco iron (78 μm) is used. As reported (Srinivas et al., 1994), using 50mm thick CT specimens tested at 298°K (room) temperature 110μm value of lc is experimentally obtained. Therefore, to validate in 3D, one-fourth FEM model of 50mm thick CT specimen using 298°K (room) temperature tensile property is created. The FEM analysis was carried out up-to the stage where maximum energy density exceeds the $E_{Fract.}$ (1357MJ/m^3). At this stage lc is obtained using the $E_{Crit.}$(92MJ/m^3) of the material at room temperature (Table 1). At critical LLD defined by $E_{Fract.}$, the highly deformed region ahead of the blunted crack front delineated by $E_{Crit.}$(92/m^3) is numerically taken as lc. At different plastic energy densities (PED), Fig. 3 showed the variation of characteristic distance across the fracture specimen thickness.

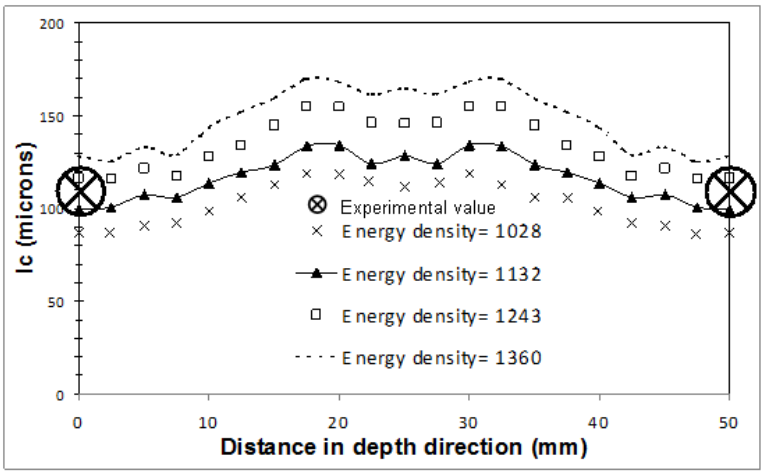

Figure 3: Validation of numerical model with experimental results (298°K)

From the figure it can be seen that the experimentally obtained lc value compares reasonably well with the numerically predicted lc value, thus validates the present numerical model. As can be seen in Fig. 3, the magnitude of 'characteristic distance' varies across the fracture specimen thickness. There is also a variation of PED magnitude across the fracture specimen thickness. Therefore, using 3D FEM models, the three possible numerical methods of predicting lc are considered in the present study. These are lc at maximum plastic energy density plane, lc at plane of minimum plastic energy density and lc near mid plane. The predicted results by

these three methods are further considered to study the dependency of lc value on temperature and fracture specimen thickness variation.

4.3 Variation of lc with fracture specimen thickness

In the present study, the variation in magnitude of characteristic distance is found due to the variation of fracture specimen thickness. There are some recommendations available in ASTM 1820 standard for obtaining valid fracture specimen parameter using the fracture specimen geometry. Based on material flow property and toughness of ductile material, ASTM has given the fracture specimen thickness criteria for obtaining valid elastic-plastic fracture parameter. Table 2 showed the variation of minimum thickness (B) requirement due to the change of temperature or flow property.

Table 2: Minimum thickness requirements and predicted lc for Armco iron tested at different temperature

Temperature (Degree Kelvin)	n	σ_y (MPa)	σ_u (MPa)	σ_f (MPa)	J_{SZW} (N/mm)	$B \geq 25 \frac{J_Q}{\sigma_f}$ (mm)	lc (mm)
298	0.29	189	296	242.5	165	17	140
383	0.30	151	338	244.5	230	23.52	116.5
423	0.41	150	385	267.5	260	24.3	79.78
473	0.48	148	404	276	290	26.27	68.41
573	0.38	146	404	275	280	25.45	119.36

The effect of fracture specimen thickness on the lc value is studied considering FEM models of CT specimen using different thicknesses (3.125mm, 6.25mm, 12.5 mm, 25mm, 50mm and 100mm thick). Considering Armco iron material tested for different temperatures, the variation of lc with fracture specimen thickness is given in Fig. 4.

It also showed the critical value of fracture specimen thickness given in ASTM code for determining geometry independent elastic plastic fracture parameter (J). From Fig. 4, it can be seen that lc becomes almost constant after a specified thickness of fracture specimen with some exceptions like results at 383°K. Similar to other critical fracture parameters (like K_{1C}, J_{1C} etc), the dependency of lc on fracture specimen thickness comes out clearly in the present study.

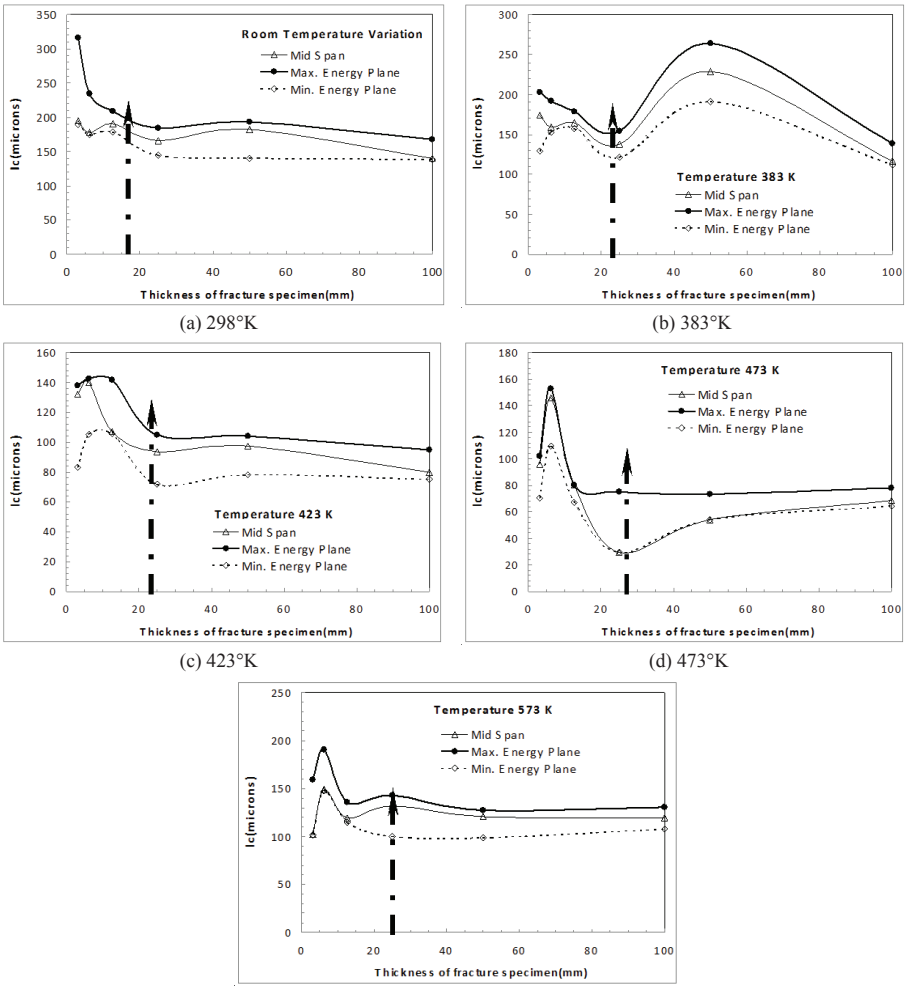

Figure 4: Variation of lc with fracture specimen thickness

4.4 Variation of lc due to temperature

To understand the variation of characteristic distance due to the change in temperature, five different tensile test results tested at five different temperatures (298°K, 383°K, 423°K, 473°K, and 573°K) are considered in the present study. At different temperatures, the variation of lc across 25mm thick CT specimen is shown in Fig. 5.

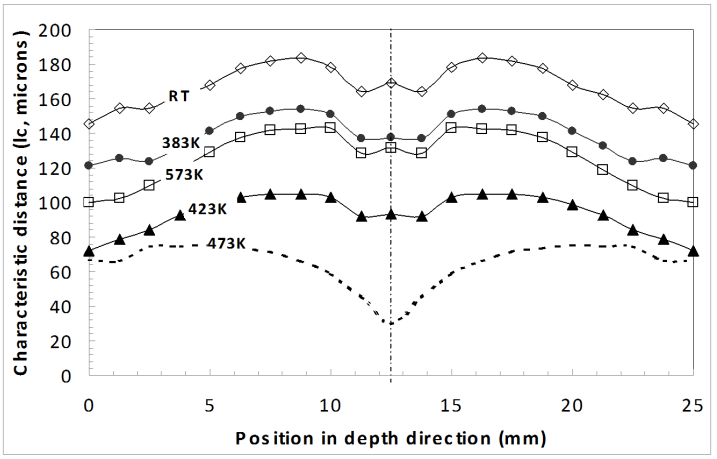

Figure 5: Variation of lc at various temperatures across the thickness (25mm)

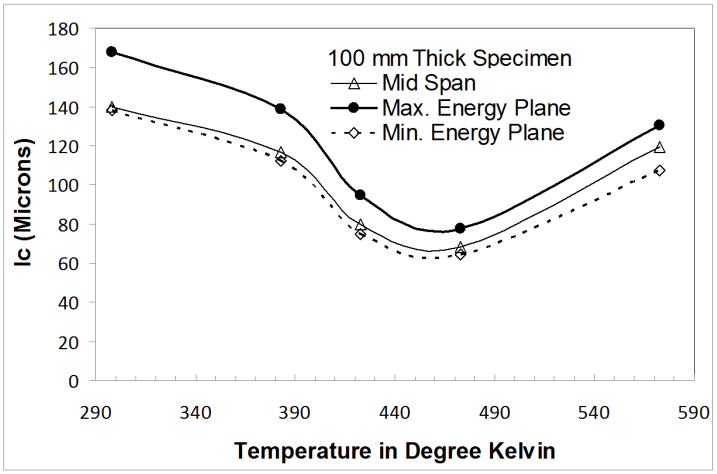

Figure 6: Variation of characteristic distance with temperature

The variation in lc values with temperature is remaining almost same across the thickness. It can be seen that across the thickness, the value of lc decreases with the increase in temperature upto 473°K, and then further increases at temperature 573°K.

Considering all the three possible lc prediction methods, the variation of lc with temperature is plotted in 100mm thick CT specimen as shown in Fig. 6.

The magnitude of lc value shown in the figure can be considered as converged

value. In all the results, the magnitude of lc reduces slowly as the temperature increases from room temperature (140-170μm) to 383°K (112-138μm) then there is a sudden decreases at temperatures 423°K (75-95μm) and at 473°K(65-75μm), which further increases to 110-130μm at 573°K. This behaviour of lc can be attributed due to dynamic strain ageing phenomenon observed in Armco iron in the temperature range 383-573°K (Srinivas, 1993).

At critical LLD, the lc value obtained at minimum PED plane in 100mm thick CT specimens is given in Table 2 for different temperatures.

5 Conclusions

The research work describes the numerical prediction of characteristic distance and its dependency on fracture specimen thickness and temperature. The present work uses three-dimensional FEM models of compact tension specimens having different thicknesses and tensile property of Armco iron tested at different temperature. The different thicknesses that were considered in the present study are 3.125mm, 6.25mm, 12.5mm, 25mm, 50mm and 100mm thick. Range of temperature that was considered in the present study varies from room temperature (298° K) to 573° K temperatures.

Following conclusion can be drawn from the present study:

- Magnitude of characteristic distance varies across the fracture specimen thickness.
- Based on the methods proposed for the numerical prediction of characteristic distance, it comes out that it depends on fracture specimen thickness and finally it converges after a specified thickness of fracture specimen.
- Characteristic distance value is also dependent on the temperature of ductile material.
- In Armco iron material, lc reduces in temperature ranges (383-573^{o}K) where dynamic strain ageing phenomenon is observed (Srinivasan, 1993) and then again increases.

References

ABAQUS Version 6.6 (2006): *User's Manual*. Rising Sun Mills Valley Street Province, RI.

ASTM standard E 1820. (2011): *Standard test method for measurement of fracture toughness.* ASTM International, PA 19428-2959, United States.

Du, J.; Thouless, M.D.; Yee, A.F. (1998): Development of a process zone in rubber-modified epoxy polymers. *Int. Jr. Frac*., vol. 92, pp. 271-285.

Hadjab, H.; Chabaat, H.S.; Thimus, J-Fr. (2007): Use of scanning electron microscope and the non-local isotropic damage model to investigate fracture process zone in notched concrete beams. *Exp. Mech*., vol. 47, pp. 473-484.

Haidar, K.; Pijaudier-Cabot, G.; Dube, J.F.; Loukili, A. (2005): Correlation between the internal length, the fracture process zone and size effect in model materials. *Mat. Struc.*, vol. 38, pp. 201-210.

Hu, X.; Duan, K. (2007): Size effect: Influence of proximity of fracture process zone to specimen boundary. *Engg. Fract. Mech*., vol. 74, no. 7, pp. 1093-1100.

Jones, J.L.; Motahari, S.M.; Varlioglu, M.; Lienert, U.; Bernier, J.V.; Hoffman, M.; U¨stu¨ndag, E. (2007): Crack tip process zone domain switching in a soft lead zirconate titanate ceramic. *Acta. Mat*., vol. 55, pp. 5538–5548.

Khedle R.; Mondal, D.P.; Verma, S.N.; Panthi S. (2011) : FEM Modeling of the Interface Strength and Its Effect on the Deformation Behaviour of Aluminum Cenosphere Syntactic Foam. *CMC:Com. Mat. & Cont.,* vol.27, no.3, pp. 211- 230.

Krasowsky, A.J.; Pluvinage, G. (1996): Minimal Resistance of Engineering Materials to Brittle Fracture as Predicted by Local Approach. *J. Phys. IV France,* vol. C6, no. 6, pp. 215-224.

Matvienko, Y.U. G. (2004): The cohesive zone model in a problem of delayed hydride cracking of zirconium alloys. *Int. Jr. Frac.,* vol. 128, pp. 73-79.

Miguel, L. F. F.; Iturrioz, I.; Riera, J. D. (2010). Size effects and mesh independence in dynamic fracture analysis of brittle materials. *Comp. Mod. Engg & Sci. (CMES),* vol. 56, no. 1, pp. 1-16.

Nakamura, S. (1995): Finite element analysis of Saint-Venant end effects in micropolar elastic solids. *Engg. Comp.,* vol. 12, pp. 571-587.

Narasaiah, N.; Tarafder, S.; Sivaprasad, S. (2010): Effect of crack depth on fracture toughness of 20MnMoNi55 pressure vessel steel. *Mat. Sci. and Engg*. vol. 527(A), pp. 2408–2411.

Orowan, E. (1948): Fracture and strength of solids. *Rep. Prog. Phys*. vol. 12, pp. 185–232.

Panthi, S. K.; Saxena, S. (2012): Prediction of Crack Location in Deep Drawing Processes Using Finite Element Simulation. *Comp., Mat., & Con.*, vol. 32, vol. 1, pp. 15-27.

Ramakrishnan, N.; Rama, R.P. (2005): An FEM study on crack tip blunting in ductile fracture initiation. *Comp. Mater. Cont*., vol. 2, no. 3, pp. 163–76.

Sanjeev, S.; Ramakrishnan, N. (2007): A comparison of micro, meso and macroscale FEM analysis of ductile fracture in a CT specimen (mode I). *Comp. Mat. Sci.,* vol. 39, pp. 1–7.

Sanjeev, S.; Ramakrishnan, N.; Chouhan, J.S. (2010): Establishing a methodology to predict the crack initiation load in through-wall cracked components using tensile specimen test data. *Int. Jr Pres. Ves. Pip.* vol. 87, pp. 737-745.

Sanjeev, S.; Ramakrishnan, N.; Dutta, B.K.(2009): Determination of stretch zone width using FEM. *Engg. Frac. Mech*., vol. 76, pp. 911–920.

Sanjeev, S.; Ramakrishnan, N.; Chouhan, J.S. (2010): Establishing methodology to predict fracture behaviour of piping components by numerically predicting specimen fracture data using tensile specimen test. *Engg. Frac. Mech*., vol. 77, pp. 1058–1072.

Sarris, E.; Papanastasiou, P. (2011): The influence of the cohesive process zone in hydraulic fracturing modeling. *Int. J. Fract*., vol. 167, pp. 33-45.

Srinivas, M.; Malakondaiah, G.; RamaRao, P. (1993): Fracture toughness of f.c.c. nickel and strain ageing b.c.c. iron in the temperature range 77–773 K. *Acta. Met. Mat.,* vol. 41, no. 4, pp. 1301–1312.

Srinivas, M.; Sundararajan, G.; Malakondaiah, G.; Rama, R.P. (1994): An analysis of ductile fracture initiation toughness in iron, its binary alloys and nickel. *Proc. Roy. Soc. Lond.*, vol. 447(A), pp. 237–51.

Tserpes, K. I.; Koumpias, A. S. (2012): Comparison between a Cohesive Zone Model and a Continuum Damage Model in Predicting Mode-I Fracture Behavior of Adhesively Bonded Joints. *Comp. Mod. Engg. & Sci.* (CMES), vol. 83, no. 2, pp. 169-181.

Vernerey, F.; Liu, W.K.; Moran, B.; Olson, G. (2009): Multi-length scale micromorphic process zone model. *Comp. Mech*., vol. 44, pp. 433-445.

Volokh, K.Y.(2011): Characteristic length of damage localization in rubber. *Int J Fract*, vol. 168, pp. 113–116.

Wang, G.Z.; Chen, J.H.; Liu, G.H. (2002): On the characteristic distance and minimum fracture toughness for cleavage fracture in a C-Mn steel. *Int. Jr. Frac*., vol. 118, pp. 57-76.

Wnuk, M.P.; Legat, J. (2002): Work of fracture and cohesive stress distribution resulting from triaxiality dependent cohesive zone model. *Int. Jr Frac.*, vol. 114, pp. 29-46.

Yang, B.; Shiva, S. (2011): Crack growth with a part-through process zone in thin plates. *Int. J. Fract*., vol. 168, pp. 145-158.

Wu, Y.; Zhang K. (2006): Crack propagation in polycrystalline elastic-viscoplastic

materials using cohesive zone models. *App. Math. Mech*., vol. 27, no. 4: 509–518.

Zhao, J.; Zhang, X. (2000): On the process zone of a quasi-static growing tensile crack with power-law elastic-plastic damage. *Int. Jr Frac*., vol. 13, pp. 383-395.

Zhiming, Y. (1998): The damage process zone characteristics at crack tip in concrete. App. Math. Mech., vol. 19, no. 1, pp. 37-43.